

## Accepted Manuscript

Climate change with elevation and its potential impact on water resources in the tianshan mountains, central Asia

Haijun Deng, Yaning Chen, Huaijun Wang, Shuhua Zhang

PII: S0921-8181(15)30052-7  
DOI: doi: [10.1016/j.gloplacha.2015.09.015](https://doi.org/10.1016/j.gloplacha.2015.09.015)  
Reference: GLOBAL 2336

To appear in: *Global and Planetary Change*

Received date: 25 March 2015  
Revised date: 16 September 2015  
Accepted date: 25 September 2015



Please cite this article as: Deng, Haijun, Chen, Yaning, Wang, Huaijun, Zhang, Shuhua, Climate change with elevation and its potential impact on water resources in the tianshan mountains, central Asia, *Global and Planetary Change* (2015), doi: [10.1016/j.gloplacha.2015.09.015](https://doi.org/10.1016/j.gloplacha.2015.09.015)

This is a PDF file of an unedited manuscript that has been accepted for publication. As a service to our customers we are providing this early version of the manuscript. The manuscript will undergo copyediting, typesetting, and review of the resulting proof before it is published in its final form. Please note that during the production process errors may be discovered which could affect the content, and all legal disclaimers that apply to the journal pertain.

1 **Climate change with elevation and its potential impact on water resources in the**  
2 **Tianshan Mountains, Central Asia**

3

4 Haijun Deng<sup>1,2</sup>, Yaning Chen<sup>1\*</sup>, Huaijun Wang<sup>1,2</sup>, Shuhua Zhang<sup>1,2</sup>

5

6 <sup>1</sup> State Key Laboratory of Desert and Oasis Ecology, Xinjiang Institute of Ecology and  
7 Geography, Chinese Academy of Sciences, Urumqi 830011, China

8 <sup>2</sup> University of Chinese Academy of Sciences, Beijing 10049, China.

9

10

11

12

13

14

15

16

17

18

19

20

21

22

23

24

25

26

---

Corresponding author: Yaning Chen

Xinjiang Institute of Ecology and Geography, CAS, No. 818 South Beijing Road, Urumqi, 830011, China.

E-mail: chenyn@ms.xjb.ac.cn, Phone: +86-0991-7823169, Fax: +86,991,7823174

27 **Abstract**

28 Climate change in complex mountain regions has an impact on the change of water  
29 resources, especially in arid areas. Here, we use long-term meteorological and  
30 hydrological station observation data to analyze the time series of climate indices and  
31 runoff to study the variability of climate in the Kaidu River Basin. The analysis results  
32 are as follows: 1) the variability rate of low temperature indices are of greater  
33 magnitude than high temperature indices; 2) overall, for the river basin, frost days and  
34 ice days all exhibited decreasing trends, and growing season lengths increased  
35 considerably; 3) during the past 50 years, overall precipitation has increased in the river  
36 basin, but there are some differences in some seasons, and precipitation from June to  
37 August accounts for approximately 66% of the annual precipitation; and 4) temperature  
38 lapse rate and precipitation of the mountain region are major factors influencing the  
39 change of runoff for the Kaidu River Basin, temperature lapse rates are the main factor  
40 influencing the run off change in the spring and fall, and precipitation in the mountain  
41 region is the major factor influencing the runoff change in the summer. Generally,  
42 climate change in complex mountain regions will be expected to seriously affect water  
43 resources in arid regions.

44 **Keywords:** Climate change; Temperature indices; Precipitation indices; Runoff analysis;  
45 Kaidu River Basin

46

47

48

49

50

51

52

53

54

## 55 **1 Introduction**

56 Climate change is a natural process of climatic systems. Climate change has received  
57 much attention in recent decades due to its effect on ecosystems and water resources.  
58 Meteorological station observation data are an important data source for studying  
59 climate change, in that they enable a better understanding of wet, dry, warm, or cool  
60 conditions, and facilitate accurate simulation of future climate change. A series of  
61 studies based on observation station data has been conducted to analyze regional climate  
62 change, e.g., in Australia (Alexander et al., 2007; Fu et al., 2010), Canada (Vincent and  
63 Mekis, 2006), China (Gemmer et al., 2004; Ding et al., 2007; Fu et al., 2013), and  
64 Europe (Rowell and Jones, 2006; Casanueva et al., 2014). These studies exhibited that  
65 air temperature showed increasing trends globally, and the precipitation change in  
66 different spatial and temporal scales has not been uniform during the past century.  
67 However, the observation stations are concentrated in low elevation regions, but are  
68 sparse in mountain regions. Mountain regions are particular geographical units and are  
69 important water resources (Immerzeel and Bierkens, 2012). In fact, almost all rivers are  
70 fed from mountain regions, and mountain regions are considered to be the “water towers  
71 of the world” (Immerzeel et al., 2010).

72 Temperature and precipitation change in mountain regions have an influence on water  
73 resource availability for downstream basins (Miller et al., 2012; Lutz et al., 2014). In  
74 complex terrain regions, the change of temperature is related to altitude (Gardner et al.,  
75 2009; You et al., 2010). Moreover, lapse rate change may affect climate model  
76 simulation results in mountain regions (Buytaert et al., 2010), especially in dry seasons  
77 (Beniston, 2003). Linear regression models of temperature and elevation were utilized  
78 to determine temperature lapse rates (Rolland, 2003; Minder et al., 2010). For example,  
79 Li et al. (2013) demonstrated that for mainland China, the temperature lapse rate  
80 exhibits a banded spatial distribution from southeast to northwest, and there are  
81 relatively large values in northwest China.

82 In examining the past 50 years, it is clear that temperature and precipitation exhibited

83 a step change in the late 1980s in the arid region of northwest China (ARNC) (Chen et  
84 al., 2014). Specifically, it has been more warm and humid in the ARNC since the  
85 mid-1980s than before the mid-1980s (Shi et al., 2002; Chen et al., 2006). Previous  
86 studies have indicated that the cold indices had significant decreases, warm indices had  
87 significant increases (Wang et al., 2013b), and most precipitation extreme indices had  
88 increasing trends (Wang et al., 2013a; Jiang et al., 2013). In the ARNC, mountain  
89 regions are important sources of water, and rivers are all supplied by the melt water in  
90 mountain regions. Moreover, climate changes in mountain regions may affect the  
91 melted water characteristics (Li et al., 2012). However, previous studies have focused  
92 on the spatial and temporal change of climate in the ARNC, and little attention has been  
93 paid to climate change with elevation.

94 In this article, we focused on the climate change with elevation in the Kaidu River  
95 Basin in the ARNC. We conducted analyses in two aspects: (1) characterizing the  
96 variability of temperature and precipitation indices with elevation in the study area; and  
97 (2) quantifying the impact of temperature lapse rate on runoff. The paper is organized as  
98 follows: Section 2 describes the study area, data collection, and methods in this study.  
99 Section 3 focuses on climate changes with elevation in the Kaidu River Basin. The  
100 discussions are provided in Section 4, and Section 5 presents the conclusions.

## 101 **2 Materials and Methods**

### 102 **2.1 Study area**

103 [Insert Figure 1 about here]

104 The Kaidu River Basin is located in the southern slope of the Tianshan Mountains and  
105 north of Yanqi Basin, is about  $4.79 \times 10^4$  km<sup>2</sup> in size largely defined by 41°47'-43°21'N  
106 and 82°58'-86°55'E, as shown in Fig. 1. From source of the Tianshan Mountain to the  
107 Bosten Lake, the length of Kaidu River is about 560 km. The water vapor in the  
108 Tianshan Mountain region is mainly controlled and affected by westerly flow (Liu et al.,  
109 2009). Therefore, the Kaidu River Basin is located in the southern slope of the Tianshan  
110 Mountains, which belongs to the leeward region. The Kaidu River originates from the

111 mountain region (i.e., higher than 5,000 m above sea level) of the Tianshan Mountains.  
112 It flows into the oasis region through the Dashankou hydrological station. The river  
113 basin in the mountains is about  $1.86 \times 10^4$  km<sup>2</sup> in size. The Kaidu River Basin includes  
114 both mountain and oasis regions. According to the variability of mean temperature,  
115 precipitation, soil, and vegetation with elevation (Table 1), the Kaidu River Basin is  
116 divided into the high mountain region (higher than 2,200 m), middle mountain region  
117 (between 1,500 m and 2,200 m), and oasis region (below 1,500 m).

118 [Insert Table 1 about here]

119 Kaidu River is one of the richest runoff rivers in the southern slope of the Tianshan  
120 Mountains. The Kaidu River Basin is an important headwater of Bosten Lake, supplying  
121 water for drinking, industrial, and agriculture use. It also has important effects on the  
122 local ecological environment and economic development. In the river basin, annual  
123 snow accumulation begins in November and ends in March (due to the daily mean  
124 temperature below 0°C in high mountains regions during this terms). Land surface  
125 temperature rises quickly in MAM (March, April, and May), and the snow-melt water  
126 supplies the Kaidu River. In JJA (June, July, and August), snow, glacial melt, and  
127 precipitation supply the Kaidu River (Fan et al., 2013).

## 128 **2.2 Data collection**

129 We collected five meteorological stations' observation data from National Climate  
130 Center (<http://ncc.cma.gov.cn>). Specifically, two of the stations are located in the large  
131 area mountain region (i.e., Bayanbulak and Balguntay), and the other stations are  
132 distributed in the oasis region (Fig. 1). The Yanqi station data for the period of record  
133 begin in 1952 and end in 2010, with the timescale of daily observation data. The  
134 Bayanbulak and Balguntay station data for the period of record are from 1958 to 2010,  
135 also with timescale of daily observation data. The Heshou and Hejing station data for  
136 the period of record are between 1960 and 2010, with the timescale of monthly  
137 observation data. Daily flow data were measured at the Dashankou hydrological station  
138 in the Kaidu River Basin for the period from 1956 to 2012 (Fig. 1). Summary details of

139 the meteorological and hydrological data for the Kaidu River Basin are provided in  
140 Table 2.

141 [Insert Table 2 about here]

## 142 **2.3 Methods**

### 143 **2.3.1 Mann-Kendal trend test**

144 The trend test is an important aspect of time series in climatic and hydrologic research.  
145 Numerous statistical tests are able to detect trends in time series data (Hamed and  
146 Ramachandra, 1998). Climatic and hydrologic time series possess some of the following  
147 characteristics: no normal data, missing values, censoring, and serial dependence. Thus,  
148 parametric statistical tests for detecting trends are commonly confounded (Hirsch and  
149 Slack, 1984). However, the Mann-Kendall trend test is a commonly used  
150 non-parametric and powerful statistical test for trend detection. Thus, it is widely used  
151 to detect long-term trends of climatic and hydrologic time series (Hirsch and Slack,  
152 1984; Hamed and Ramachandra, 1998; Kahya and Kalayci, 2004; Chen and Xu, 2005).  
153 The three steps of the Mann-Kendall test are as follows: 1) according to the  $n$  time  
154 series value  $x_1, x_2, x_3, \dots, x_n$ , calculate their relative rank  $r_i$  ( $i=1, 2, 3, \dots, n$ ); 2) calculate  
155 statistic  $Z$  value,  $Z = |S|/\alpha^{0.5}$ ; and 3) if  $Z > Z_{\alpha/2}$ , then the trend is significant at the  
156 level of  $\alpha$ . A positive value of  $S$  indicates an upward trend, and a negative value  
157 indicates a downward trend.

### 158 **2.3.2 Climate indices**

159 Climate indices are calculated from acquired temperature and precipitation daily  
160 observation data. In the study area, the timescales of the Bayanbulak, Balguntay, and  
161 Yanqi are daily observation data. These stations are part of the national standard  
162 meteorological station system, whose observations time series are continuous and  
163 without missing values. Therefore, these stations are representative in each elevation  
164 band. So, we have chosen the three meteorological stations that were consistently  
165 available for the period from 1958 to 2010 (Fig. 1 and Table 1). Using these data, we

166 calculated all of the 15 temperature and precipitation indices supported by RClimDex  
 167 (1.1) (<http://etccdi.pacificclimate.org/software.shtml>) and Matlab (R2013a), including  
 168 10 indices (TNn, TXx, FDO, IDO, SU25, GSL, Pav, CWD, CDD, and R10) by  
 169 RClimDex (1.1) and five indices (TNm, TMn, Tav, TMx, and TXm) by Matlab code.  
 170 Details regarding temperature and precipitation indices (including ID, name, definitions,  
 171 and units) are presented in Table 3.

172 [Insert Table 3 about here]

### 173 **2.3.3 Temperature lapse rate**

174 Linear regression models are utilized to analyze variability of temperature with  
 175 elevation (Kattel et al., 2013; Chiu et al., 2014). There is an estimated error when the  
 176 lapse rate was calculated using the estimated linear regression model. Harlow et al.  
 177 (2004) used a 10 day running mean of the temperature to eliminate a possible estimated  
 178 errors effect. In this research, we employed the monthly running mean of the mean  
 179 temperature to exclude the possibility of an estimated errors effect.

180 To compute the temperature lapse rate, we chose station data of the period from 1960  
 181 to 2010. The linear regression model, shown in equation (1), was used to compute  
 182 temperature lapse rates in different altitude regions:

$$183 \quad T = a - tlr * \Delta H \quad (1)$$

184 where  $T$  is the temperature at a second location;  $a$  is the temperature at the base location,  
 185 which is here the temperature of the oasis region stations;  $tlr$  is the temperature lapse  
 186 rate ( $^{\circ}\text{C}/\text{km}$ ); and  $\Delta H$  is the difference in altitude between the two locations.

187 Then,

$$188 \quad tlr = (a - T) / \Delta H \quad (2)$$

189 where  $tlr$  is the temperature lapse rate ( $^{\circ}\text{C}/\text{km}$ );  $T$  is the temperature at the second  
 190 location;  $a$  is the temperature at the base location; and  $\Delta H$  is the difference in altitude.  
 191 In this study, we will utilize the temperature lapse rate at annual and monthly scales.

192 Pearson's correlation test (Chen et al., 2014) was employed to analyze the  
 193 correlations of the runoff with temperature lapse rate and precipitation.



### 194 2.3.4 Agriculture and urbanization contributions

195 Climate changes are different in mountain and oasis regions. Mountain region  
 196 temperature change is mostly derived from natural forcing. However, temperature  
 197 change in oasis region may not accurately reveal the true nature of temperature  
 198 variability, because urban and agricultural areas are concentrated in oasis regions.  
 199 Therefore, agriculture and urbanization effects are computed by using the following  
 200 equation (Zhou et al., 2009):

$$201 \Delta T_{ca} = T_o - T_m \quad (3)$$

202 where  $\Delta T_{ca}$  is the agriculture and urbanization effects;  $T_o$  is the temperature trend in the  
 203 oasis region, which is caused by natural and anthropogenic activity forcing; and  $T_m$  is  
 204 the temperature trend in the mountain region and represents natural variability.  
 205 Therefore,  $\Delta T_{ca}$  is the temperature variability due to anthropogenic activity forcing.  
 206 Then, agriculture and urbanization are calculated by the following equation:

$$207 \beta = \Delta T_{ca} / |T_o| \quad (4)$$

208 where  $\beta$  is the contribution of agriculture and urbanization;  $|T_o|$  is absolute value of  $T_o$ .  
 209 When (1)  $\beta > 0$ , then the contribution of agriculture and urbanization is positive; (2)  $\beta = 0$   
 210 indicates that the contribution of agriculture and urbanization is insignificant; and (3)  $\beta$   
 211  $< 0$  shows that the contribution of agriculture and urbanization is negative.

## 212 3 Results

### 213 3.1 Climatic indices

#### 214 3.1.1 Temperature indices

215 The trend analysis indicated that the mean air temperature ( $T_{av}$ ) in the Kaidu River  
 216 Basin increased in the past 53 years. In the upward directions,  $T_{av}$  had statistically  
 217 significant positive trends in the oasis region and middle mountain region, and was  
 218 significant at  $p < 0.01$ , with rates of  $0.037$  and  $0.036^\circ\text{C}/\text{a}$ , respectively. In the high  
 219 mountain region an increasing trend was observed for  $T_{av}$ ; however, it was only  
 220 significant at the  $0.05$  level, and the rate was  $0.023^\circ\text{C}/\text{a}$ .

221 [Insert Figure 2 about here]

222 Figure 2 clearly shows the variability of the daily temperature indices in these three  
223 sub-regions. In the oasis region, among the daily temperature indices (Min Tmin, Mean  
224 Tmin, Min Tmean, Mean Tmean, Max Tmean, Mean Tmax, and Max Tmax), the  
225 increasing rate of Min Tmin ( $4.2^{\circ}\text{C}/50\text{a}$ ) was the strongest, followed by those of Mean  
226 Tmin ( $2.53^{\circ}\text{C}/50\text{a}$ ), Min Tmean ( $3.51^{\circ}\text{C}/50\text{a}$ ), Mean Tmean ( $1.82^{\circ}\text{C}/50\text{a}$ ), Max Tmean  
227 ( $1.29^{\circ}\text{C}/50\text{a}$ ), Mean Tmax ( $0.79^{\circ}\text{C}/50\text{a}$ ), and Max Tmax ( $0.59^{\circ}\text{C}/50\text{a}$ ). In the middle  
228 mountain region, among the daily temperature indices, the increasing rate of Mean  
229 Tmin ( $3.61^{\circ}\text{C}/50\text{a}$ ) was the strongest, and only the Max Tmax variability rate of  $-0.54^{\circ}\text{C}$   
230 /50a became a decreasing trend. In the high mountain region, the increasing rate of Min  
231 Tmin ( $1.56^{\circ}\text{C}/50\text{a}$ ) was the strongest, and the variability rate of Max Tmax ( $-0.33^{\circ}\text{C}/50\text{a}$ )  
232 was the lowest.

233 [Insert Figure 3 about here]

234 The summer and winter variability rates of the temperature indices are shown in Fig.  
235 3. In summer, only the variability rate of Max Tmax ( $-0.54^{\circ}\text{C}/50\text{a}$ ) in the middle  
236 mountain region showed a decreasing trend, and the other temperature indices showed  
237 increasing trends. The increasing rate of Mean Tmin ( $3.71^{\circ}\text{C}/50\text{a}$ ) in the middle  
238 mountain region was the largest (Fig. 3A). Moreover, the variability rate of the  
239 temperature indices in winter exhibited increasing trends (except the Max Tmax  
240 decreasing trend in the oasis region); whereas, the increasing rate of Min Tmin ( $4.2^{\circ}\text{C}$   
241 /50a, in the oasis region) was larger than the other regions (Fig. 3B).

242 The variability rate of low temperature indices (Min Tmin, Mean Tmin, and Min  
243 Tmean) had a stronger trend than high temperature indices (Max Tmean, Mean Tmax,  
244 and Max Tmax) in the Kaidu River Basin (Fig.2 and 3). At the same time, it can be seen  
245 that the range of variability of temperature indices in the high mountain region showed  
246 relative stability, and were less than the variability range of temperature indices in the  
247 middle mountain region and oasis region.

248 Table 4 presents the trend analysis results of frost days (FDO), ice days (IDO), and

249 summer days (SU25) in the Kaidu River Basin. The frost days had significant  
250 decreasing trends in all three sub-regions (i.e., oasis region, middle mountain region,  
251 and high mountain region), with rates of -0.38 day/a, -0.59 day/a, and -0.37 day/a,  
252 respectively. The trend of ice days for the three sub-regions was not significant at the  
253 0.05 level. Summer days had positive trends in the oasis region (at the level of 0.01) and  
254 middle mountain region (at the level of 0.05). However, the trend of summer days for  
255 the high mountain region was not significant at the level of 0.05, and this may be related  
256 to a characteristic of high mountain region (i.e., in these regions, which are above 2200  
257 m, days in which the daily maximum temperature is greater than 25°C are relatively  
258 rare).

259 [Insert Table 4 about here]

260 [Insert Figure 4 about here]

261 Analysis results show that frost days had a significant decreasing trend, and summer  
262 days had a significant increasing trend in the Kaidu River Basin during the past 50 years,  
263 indicating that the accumulated temperature (the sum of mean temperature  $\geq 10^{\circ}\text{C}$ ) for  
264 cultivation increased in the local area. Consequently, the changes of accumulated  
265 temperature for cultivation would affect the length of growing seasons. Figure 4 reveals  
266 positive increasing trends of growing season length (GSL) in the high mountain region,  
267 the middle mountain region, and the oasis region. After the late 1980s, the GSL had  
268 significant increasing trends in the middle mountain region and oasis region (Fig. 4).  
269 Although longer GSLs will increase crop areas and yield in the local region, it will also  
270 tend to strain the water resource supply.

### 271 3.1.2 Precipitation indices

272 In the Kaidu River Basin, most precipitation is concentrated from May to September,  
273 with high air temperature occurring during this period. To analyze seasonally variability,  
274 annual precipitation was calculated for the past 50 years, as shown in Fig. 5A-C. Figure  
275 5 shows that JJA (from June to August) precipitation accounts for approximately 66% of  
276 the annual precipitation in the three sub-regions (i.e., oasis region, middle mountain

277 region, and high mountain region). In spring time, the proportion of MAM (from March  
278 to May) precipitation exhibited an increasing trend from 1958 to 2010 in the oasis  
279 region, while it showed decreasing trends in the mountain region. In summer, the  
280 proportion of JJA precipitation in the annual precipitation had a decreasing trend in the  
281 oasis region, and had an increasing trend in the middle mountain region; however, the  
282 change trend of the proportion of JJA precipitation is not obvious. In autumn, the  
283 proportion of SON (from September to November) precipitation in the annual  
284 precipitation was approximately 14%. It exhibited increasing trends in the oasis and  
285 high mountain regions, and had a decreasing trend in the middle mountain region.

286 [Insert Figure 5 about here]

287 In the oasis region, the rise of precipitation in MAM and SON are major contributors  
288 to the rise of annual precipitation during the past 50 years (Fig. 5A). The annual  
289 precipitation reveals that the significant increase of the middle mountain region was  
290 caused by the significant increase of precipitation in JJA (Fig. 5B). In the mountain  
291 region, however, the increase of precipitation in SON and JFD contributed most to the  
292 increase of annual precipitation (Fig. 5C).

293 Based on these results, it can be concluded that the wet trend began in the mid-1980s  
294 in the Kaidu River Basin. However, precipitation showed similar negative anomalies  
295 after the 2000s in the middle mountain region (Fig. 5B) and the oasis region (Fig. 5A);  
296 whereas, a positive anomaly appeared in the high mountain region (Fig. 5C).

297 [Insert Figure 6 about here]

298 Precipitation exhibited an increasing trend (about 6.6 mm/10a) in the Kaidu River  
299 Basin during the past 50 years. The R10 and CWD had increasing trends, with rates of  
300 0.16 day/10a and 0.07 day/10a, respectively. Figure 6 shows correlations between  
301 annual precipitation and R10 and CWD over the period of 1958 to 2010. It indicated  
302 that there are significant linear correlations between annual precipitation and R10  
303 ( $R^2=0.67$ ,  $P<0.01$ ) and CWD ( $R^2=0.27$ ,  $p<0.01$ ). The R10 and CWD are extreme  
304 precipitation indices, and the R10 is an intensity indices and CWD is a consecutive

305 indices. At the same time, the climate extremes are closely related to the climate average  
306 state during the past 50 years in the arid region of the northwest China. Meanwhile, the  
307 relationship with R10 is stronger and CWD is weaker. This may be due to that the R10  
308 had a relatively strong increasing trend (i.e., 0.16 day/10a) higher than CWD (i.e., 0.07  
309 day/10a) during the past 50 years. The significant linear correlation indicates that there  
310 is adequate evidence to conclude that the R10 and CWD were major factors in the rise  
311 of precipitation during the past 50 years in the Kaidu River Basin.

### 312 **3.2 Temperature lapse rate**

313 Figure 7A presents the annual mean temperature lapse rate for our observation station  
314 data. The annual mean temperature lapse rate (tlr) is  $-8.6\text{ }^{\circ}\text{C}/\text{km}$ , indicating that the  
315 mean temperature lapse rate of the Kaidu River Basin is steeper than the free-air moist  
316 adiabatic lapse rate (about  $-6.5\text{ }^{\circ}\text{C}/\text{km}$ ) and closer to the dry adiabatic lapse rate ( $-9.8\text{ }^{\circ}\text{C}$   
317  $/\text{km}$ ). From figure 7b, it can be seen that the largest monthly mean temperature lapse  
318 rate occurs in February, and the smallest monthly mean temperature lapse rate occurs in  
319 October. The seasonal variability of the mean temperature lapse rate decreased in  
320 summer and then increased in winter. Therefore, the winter half-year mean temperature  
321 lapse rate was steeper than the summer half-year.

322 [Insert Figure 7 about here]

323 The year-to-year variability is then examined by analyzing the distribution of the  
324 monthly mean temperature lapse rate calculated from the observation station data from  
325 1958 to 2010. Specifically, the median, inner-quartile range (IQR), full range and  
326 extremes of monthly mean temperature lapse rate are identified, as shown in Fig. 7B.  
327 The IQR is equal to the difference between the upper and lower quartiles ( $\text{IQR}=\text{Q3}-\text{Q1}$ );  
328 the IQR shows the mean temperature lapse rate typical variations, which varies from  
329  $0.436\text{ }^{\circ}\text{C}/\text{km}$  (Jul) to  $3.427\text{ }^{\circ}\text{C}/\text{km}$  (Dec). The full range of monthly mean temperature  
330 lapse rate is smallest in summer (Jun-Aug) and largest in winter (Dec-Feb) (Fig. 7B). In  
331 addition, year-to-year variability of the monthly mean temperature lapse rate in some  
332 years was even steeper than  $-10\text{ }^{\circ}\text{C}/\text{km}$  (steeper than the dry adiabatic lapse rate) in

333 Jan-Mar. These differences may be affected by local climatic features, such as the  
334 seasonal cycle of snow cover in mountain regions, cold air masses from  
335 Siberia-Mongolia, and local circulation.

### 336 **3.3 Runoff analysis**

337 Figure 8A shows the change characteristics of runoff for yearly and seasonal scales in  
338 the Kaidu River Basin. Results from this figure indicate that the runoff in summer (JJA)  
339 was the largest and was greater than other seasons (i.e., MAM, SON, and JFD). At the  
340 same time, the runoff had a significant increasing trend in the mid-1980s to 2000;  
341 however, this trend did not continue on or after the year 2000. Figure 8B shows  
342 year-to-year variability in monthly mean runoff from 1956 to 2012 of the Kaidu River  
343 Basin. From this figure, we can see that the variability of monthly mean runoff was  
344 larger during the summer months (Jun, Jul, and Aug) than the winter months (Dec, Jan,  
345 and Feb). These differences may indicate that the main sources of runoff are base-flow  
346 in the winter, and glacier meltwater and precipitation in the summer (Fan et al., 2013).  
347 Moreover, the inter-annual variability of base-flow is less than the precipitation.

348 [Insert Figure 8 about here]

349 Figure 9 shows comparisons between the change of runoff and change of temperature  
350 lapse rates and precipitation. Results from the comparison analysis indicated that for the  
351 change of runoff, temperature lapse rates play an important role in the Kaidu River  
352 Basin (Fig. 9A). It is clearly seen that the runoff will have a lower flow period during  
353 steeper temperature lapse rate value periods (i.e., in the 1970-2000 year) during the past  
354 50 years, and vice versa. The reason of reverse changes in the 1970-2000 is the steeper  
355 temperature lapse rates will lead to lower air temperature in the higher mountain region,  
356 which decreases the runoff. Figure 9B shows that the relationship between runoff and  
357 precipitation is positively correlated over the past 50 years, and the correlation  
358 coefficient values (Table 5) indicated that the runoff has a significant positive  
359 correlation with precipitation in MAN ( $R^2=0.28$ ,  $p<0.05$ ) and in JJA ( $R^2=0.75$ ,  $P<0.01$ ).  
360 From Table 5, it can be seen that temperature lapse rates are a dominant factor affecting

361 the runoff in MAM and SON, and precipitation is the major factor for the runoff in the  
362 summer; whereas, in winter, the temperature lapse rates and precipitation contribution  
363 were much less. Identifying these relationships will help us to elucidate how  
364 temperature lapse rates and precipitation changes could affect runoff in the Kaidu River  
365 Basin.

366 [Insert Figure 9 about here]

367 [Insert Table 5 about here]

#### 368 **4 Discussion**

369 In this paper, detailed analyses are performed regarding the variability of climatic  
370 indices with elevation in the Kaidu River Basin during the past 50 years.

371 The results showed that the low temperature indices change at a greater rate than the  
372 high temperature indices. This may be due to that the large scale atmospheric circulation  
373 (i.e., wind field, Siberian High index) (Li et al., 2012; You et al., 2011) and human  
374 activity (Fig.10) lead to cold extremes decreased faster (Wang et al., 2013c). At the  
375 same time, the oasis region temperature has been rising faster than that in the mountain  
376 region. This may be due to that human activity (i.e., cities and agricultural activity) is  
377 concentrated in the oasis region. For instance, from 1990 to 2010, the agricultural land  
378 area increased from 2269.19 km<sup>2</sup> to 3804.34 km<sup>2</sup>, an increase of 67.6%; while  
379 residential and industrial land grew from 208.64 km<sup>2</sup> to 306.76 km<sup>2</sup>, an increase of 47%  
380 (Wang et al., 2014). The cities and agricultural activities for the Tmean, Tmin and Tmax  
381 of the oasis region (Fig.10) exhibited increases of 0.029 °C/10a, 0.08 °C/10a and  
382 0.064 °C/10a, respectively. So, the cities and agricultural contribution to the Tmean  
383 increase is 8.8%, to the Tmin increase is 15.7%, and to the Tmax increase is 22.9%.  
384 Human activities (i.e., agriculture, residential, and industrial) on a large scale tend to  
385 produce aerosols and greenhouse gases, with consequent strong effects on temperature  
386 change (Mahlstein and Knutti, 2010). Thus, the extension of cities and agriculture areas  
387 will contribute to the temperature increases in the oasis region during the past score  
388 years. Therefore, the impact of human factors on natural factors results in the air

389 temperature showing significantly increasing trends in the oasis region (Chen et al.,  
390 2013; Tao et al., 2011; Xu et al., 2008).

391 [Insert Figure 10 about here]

392 Topographical effects are important factors in the variations of temperature indices  
393 with elevation. One possible reason for this may be due to the large area glaciers and  
394 seasonal snow cover in the high mountain region. Seasonal glaciers and snow melt will  
395 lead to increases in high mountain region soil moisture, which will cause temperature  
396 changes to exhibit relative stability in the high mountain region.

397 In addition, topography and snow cover are the main factors affecting the variability  
398 of the temperature lapse rate in the Kaidu River Basin. Some researchers have  
399 recognized that temperature lapse rate variability may be influenced by local climate  
400 features (Minder et al., 2010; Kattel et al., 2013; Chiu et al., 2014), such as the seasonal  
401 cycle of snow cover in mountain regions, cold air masses, and local circulation. The  
402 results of the present study indicated that the temperature lapse rate (i.e.,  $-8.6^{\circ}\text{C}/\text{km}$ ) is  
403 steeper than  $-6.5^{\circ}\text{C}/\text{km}$  (free-air moist adiabatic lapse rate); in some months (Jan, Feb,  
404 and Mar), it is even steeper than  $-10^{\circ}\text{C}/\text{km}$ . This may be due to that the Kaidu River  
405 Basin is located in the southern slope of the Tianshan Mountains, which belongs to the  
406 leeward side region. So, the dry air in the leeward side region during these months (Jan,  
407 Feb, and Mar), and the air-upward process with elevation is similar to the dry-adiabatic  
408 process. On the other hand, the high mountain region has a larger area snow and  
409 glaciers cover, which exerts a cooling effect due to the albedo increase (Groisman et al.,  
410 1994). At the same time, the low altitude region (i.e., the oasis region) is located in the  
411 Yanqi Basin with terrain occlusion, resulting in obstruction of cold air in winter.

412 In mountainous regions, the temperature lapse rate is a sensitive factor that affects  
413 snowmelt runoff (Jain et al., 2010; Minder et al., 2010). The Kaidu River runoff is an  
414 important water resource in the local area. The Kaidu River sources of replenishment of  
415 runoff are melt water (snow and glacial) and precipitation (Fan et al., 2013). And  
416 different runoff formats affected by climate factors are different in the Kaidu River



417 Basin. Fan et al., (2013) suggest that precipitation processes have impact on quick flow,  
418 and temperature processes on baseflow. Meanwhile, the solid precipitation (i.e., snow)  
419 present in the winter half-years will supply the river runoff and underground water when  
420 the air temperature rises in the late-spring and summer months. The results of the  
421 analysis also revealed that the effects of temperature lapse rates on runoff are complex  
422 in the Kaidu River Basin, which may be due to the complex correlations between  
423 temperature lapse rate and snow melt water and precipitation. For example, in the MAM,  
424 the runoff had a significant positive correlation with temperature lapse rates. This may  
425 be due to the rise of spring temperature, which makes the runoff increase with the snow  
426 melt water increase in the mountain regions. Nevertheless, there was a significant  
427 negative correlation between runoff and temperature lapse rates in the SON. This is due  
428 to that the precipitation in the annual precipitation was approximately 14% (Fig. 8a) in  
429 autumn; thus, glacier and snow melt water are major sources of the river runoff.  
430 Therefore, the temperature lapse rate is an important factor in the runoff change during  
431 autumn. Specifically, this is because the troposphere of direct heat sources comes from  
432 near surface long-wave radiation. So, steeper temperature lapse rates will lead to lower  
433 air temperature in the higher mountain region, which decreases the runoff; conversely,  
434 shallower temperature lapse rates will cause higher air temperature in the higher  
435 mountain region, which increases the runoff. Thus, when the mountain region warms  
436 (cools), the glacier and snow melt water will correspondingly increase (decrease).  
437 Therefore, the temperature lapse rates determine the runoff by strongly influencing the  
438 snow and glacier melt in the mountain regions.

439 The present study has largely focused on analyzing how temperature lapse rates affect  
440 runoff variability. This research contains one limitation in that how well each station  
441 represents its entire elevation band cannot be ascertained due to the use of only one  
442 station in each band. However, this work makes a unique contribution to the literature,  
443 in that it utilized empirical equations based on data from five stations to calculate  
444 temperature lapse rates. On the one hand, based on the previous literature, lapse rate and

445 runoff are not sufficient to interpret the relationship between climate extremes. On the  
446 other hand, there are a series of factors, i.e., temperature, topographic features and local  
447 circulation patterns, which have affected temperature lapse rate variability. Therefore,  
448 identifying the influence of these factors on temperature lapse rate variability will  
449 constitute an important aspect of our next research.

## 450 **5 Conclusions**

451 In this study, the variability of temperature and precipitation indices with elevation were  
452 analyzed in the Kaidu River Basin based on daily observation data during the past 50  
453 years. From the results, we conclude that runoff characteristics are affected by  
454 temperature lapse rate changes in the Kaidu River Basin.

455 During the past 50 years, the air temperature had significant positive trends in the  
456 study area; moreover, the increasing rate of temperature in the oasis region was higher  
457 than the mountain region. At the same time, we discovered that the rising rate of low  
458 temperature indices was larger than the high temperature indices. With the daily  
459 minimum temperature increasing, the growing season length exhibited a significant  
460 increasing trend after the late 1980s. There are also differences of seasonal variability  
461 for precipitation in these three sub-regions. It was found that heavy precipitation days  
462 (R10) and maximum consecutive wet days (CWD) contributed most to the increasing  
463 precipitation.

464 Snow and glacier melt are important water source supplies of runoff for mountain  
465 regions, and changes in temperature lapse rates have significant effects on runoff  
466 characteristics. Therefore, the temperature lapse rate should be viewed as critical factor  
467 when forecasting and simulating the runoff change of mountain regions in the future.

468

## 469 **Acknowledgements:**

470 The research is supported by the Program of the State Key Laboratory of Desert and

471 Oasis Ecology, Xinjiang Institute of Ecology and Geography, Chinese Academy of  
472 Sciences (Y371163), and the National Natural Science Foundation of China (41471030).  
473 The authors would like to thank National Climate Central, China Meteorological  
474 Administration, for generously providing the meteorological data for this study. The  
475 authors appreciate comments provided and encouragement made by the reviewers, the  
476 editor and the associate editor.

477 **References:**

- 478 Alexander, L.V., Hope, P., Collins, D., Trewin, B., Lynch, A., Nicholls, N., 2007. Trends  
479 in Australia's climate means and extremes: a global context. *Aust. Meteorol. Mag.*,  
480 56(1): 1-18.
- 481 Beniston, M., 2003. *Climate Variability and Change in High Elevation Regions: Past,*  
482 *Present & Future*, Springer Netherlands, pp. 5-31. DOI:  
483 10.1007/978-94-015-1252-7\_2.
- 484 Buytaert, W., Vuille, M., Dewulf, A., Urrutia, R., Karmalkar, A., Célleri, R., 2010.  
485 Uncertainties in climate change projections and regional downscaling:  
486 implications for water resources management. *Hydrol. Earth. Syst. Sc.*, 7(2):  
487 1247-1258. DOI: 10.5194/hess-14-1247-2010.
- 488 Casanueva, A., Rodríguez-Puebla, C., Frías, M.D., González-Reviriego, N., 2014.  
489 Variability of extreme precipitation over Europe and its relationships with  
490 teleconnection patterns. *Hydrol. Earth. Syst. Sc.*, 18(2): 709-725. DOI:  
491 10.5194/hess-18-709-2014.
- 492 Chen, Y.N., Xu, Z.X., 2005. Plausible Impact of Globe Climate Change on Water  
493 Resources in the Tarim River Basin, China. *Sci. China Ser. D*, 48(1):65-73. DOI:  
494 10.1360/04yd0539.
- 495 Chen, Y.N., Takeuchi, K., Xu, C.C., Chen, Y.P., Xu, Z.X., 2006. Regional climate change  
496 and its effects on river runoff in the Tarim Basin, China. *Hydrol. Process.*,  
497 20(10):2207-2216. DOI:10.1002/hyp.6200.
- 498 Chen, Y., Deng, H., Li, B., Li, Z., Xu, C., 2014. Abrupt change of temperature and

- 499 precipitation extremes in the arid region of Northwest China. *Quatern. Int.*, 336:  
500 35-43. DOI: 10.1016/j.quaint.2013.12.057
- 501 Chen, Z., Chen, Y., Li, B., 2013. Quantifying the effects of climate variability and  
502 human activities on runoff for Kaidu River Basin in arid region of northwest  
503 China. *Theor. Appl. Climatol.*, 111(3-4): 537-545. DOI:  
504 10.1007/s00704-012-0680-4.
- 505 Chiu, C.A., Lin, P.H., Tsai, C.Y., 2014. Spatio-Temporal Variation and Monsoon Effect  
506 on the Temperature Lapse Rate of a Subtropical Island. *Terr. Atmos. Ocean. Sci.*,  
507 25(2): 203-217. DOI: 10.3319/tao.2013.11.08.01(a).
- 508 Ding, Y., Ren, G., Zhao, Z., Xu, Y., Luo, Y., Li, Q., Zhang, J., 2007. Detection, causes  
509 and projection of climate change over China: An overview of recent progress.  
510 *Adv. Atmos. Sci.*, 24(6): 954-971. DOI: 10.1007/s00376-007-0954-4.
- 511 Fan, Y., Chen, Y., Liu, Y., Li, W., 2013. Variation of baseflows in the headstreams of the  
512 Tarim River Basin during 1960–2007. *J. Hydrol.*, 487: 98-108. DOI:  
513 10.1016/j.jhydrol.2013.02.037.
- 514 Fu, G., Viney, N.R., Charles, S.P., Liu, J., 2010. Long-term temporal variation of  
515 extreme rainfall events in Australia: 1910-2006. *J. Hydrometeorol.*, 11(4): 950-965.  
516 DOI: <http://dx.doi.org/10.1175/2010JHM1204.1>.
- 517 Fu, G.B., Yu, J.J., Yu, X.B., Ouyang, R.L., Zhang, Y.C., Wang, P., Liu, W.B., Min, L.L.,  
518 2013. Temporal variation of extreme rainfall events in China, 1961-2009. *J.*  
519 *Hydrol.*, 487: 48-59. DOI: 10.1016/j.jhydrol.2013.02.021.
- 520 Gardner, A.S., Sharp, M.J., Koerner, R.M., Labine, C., Boon, S., Marshall, S.J., Burgess,  
521 D.O., Lewis, D., 2009. Near-surface temperature lapse rates over Arctic glaciers  
522 and their implications for temperature downscaling. *J. Climate*, 22(16):  
523 4281-4298. DOI: 10.1175/2009JCLI2845.1.
- 524 Gemmer, M., Becker, S., Jiang, T., 2004. Observed monthly precipitation trends in  
525 China 1951–2002. *Theor. Appl. Climatol.*, 77(1-2): 39-45. DOI:  
526 10.1007/s00704-003-0018-3.

- 527 Groisman, P.Y., Karl, T.R., Knight, R.W., Stenchikov, G.L., 1994. Changes of Snow  
528 Cover, Temperature, and Radiative Heat Balance over the Northern Hemisphere,  
529 J. Climate, 7(11):1633-1656. DOI: 10.1175/1520-0442(1994)007.
- 530 Hamed, K.H., Ramachandra, R. A., 1998. A modified Mann-Kendall trend test for  
531 autocorrelated data. *J.Hydrol.*, 204(1-4): 182-196. DOI:  
532 10.1016/S0022-1694(97)00125-X.
- 533 Hirsch, R.M., Slack, J.R., 1984. A Nonparametric trend test for seasonal data with serial  
534 dependence. *Water Resour. Res.*, 20(6): 727-732. DOI:  
535 10.1029/WR020i006p00727.
- 536 Immerzeel, W.W., Van Beek, L.P.H., Bierkens, M.F.P., 2010. Climate change will affect  
537 the asian water towers. *Science*, 328(5984): 1382-1385. DOI:  
538 10.1126/science.1183188.
- 539 Immerzeel, W.W., Bierkens, M.F.P., 2012. Asia's water balance. *Nat.Geosci.*, 5(12):  
540 841-842. DOI:10.1038/ngeo1643.
- 541 Jain, S.K., Goswami, A., Saraf, A.K., 2010. Snowmelt runoff modelling in a Himalayan  
542 basin with the aid of satellite data. *Int.J.Remote Sens.*, 31(24): 6603-6618. DOI:  
543 10.1080/01431160903433893.
- 544 Jiang, F.Q., Hu, R.J., Wang, S.P., Zhang, Y.W., Tong, L., 2013. Trends of precipitation  
545 extremes during 1960–2008 in Xinjiang, the Northwest China.  
546 *Theor.Appl.Climatol.*, 111(1-2): 133-148. DOI: 10.1007/s00704-012-0657-3.
- 547 Kahya, E., Kalayci, S., 2004. Trend analysis of streamflow in Turkey. *J.Hydrol.*,  
548 289(1-4): 128-144. DOI: 10.1016/j.jhydrol.2003.11.006.
- 549 Kattel, D.B., Yao, T., Yang, K., Tian, L., Yang, G., Joswiak, D., 2013. Temperature lapse  
550 rate in complex mountain terrain on the southern slope of the central Himalayas.  
551 *Theor. Appl.Climatol.*, 113(3-4): 671-682. DOI: 10.1007/s00704-012-0816-6.
- 552 Li, B., Chen, Y., Chen, Z., Li, W., 2012. The Effect of Climate Change during Snowmelt  
553 Period on Streamflow in the Mountainous Areas of Northwest China. *Acta*  
554 *Geographica Science* 67(11): 1461-1470. DOI: 10.11821/xb201211003.

- 555 Li, B., Chen, Y. and Shi, X., 2012. Why does the temperature rise faster in the arid  
556 region of northwest China? *Journal of Geophysical Research: Atmospheres*,  
557 117(D16), D16115. DOI: 10.1007/s00704-012-0816-6.
- 558 Li, X., Wang, L., Chen, D., Yang, K., Xue, B., Sun, L., 2013. Near-surface air  
559 temperature lapse rates in the mainland China during 1962-2011. *J. Geophys. Res.*,  
560 118(14): 7505-7515. DOI: 10.1002/jgrd.50553.
- 561 Liu, J.R., Song, X.F., Sun, X.M., Yuan, G.F., Liu, X., Wang, S.Q., 2009. Isotopic  
562 composition of precipitation over Arid Northwestern China and its implications  
563 for the water vapor origin. *J. Geogr. Sci.*, 19 (2):164–174. DOI:  
564 10.1007/s11442-009-0164-3.
- 565 Lutz, A.F., Immerzeel, W.W., Shrestha, A.B., Bierkens, M.F.P., 2014. Consistent  
566 increase in High Asia's runoff due to increasing glacier melt and precipitation.  
567 *Nat. Clim. Change*, 4(7):587-592. DOI: 10.1038/NCLIMATE2237.
- 568 Mahlstein, I., Knutti, R., 2010. Regional climate change patterns identified by cluster  
569 analysis, *Clim. Dynam.*, 35(4):587-600. DOI: 10.1007/s00382-009-0654-0.
- 570 Miller, J.D., Immerzeel, W.W., Rees, G., 2012. Climate Change Impacts on Glacier  
571 Hydrology and River Discharge in the Hindu Kush–Himalayas. *Mt. Res. Dev.*,  
572 32 (4): 461-467.
- 573 Minder, J.R., Mote, P.W., Lundquist, J.D., 2010. Surface temperature lapse rates over  
574 complex terrain: Lessons from the Cascade Mountains, *J. Geophys. Res.*, 115:  
575 D14122. DOI: 10.1029/2009JD013493.
- 576 Rowell, D., Jones, R., 2006. Causes and uncertainty of future summer drying over  
577 Europe. *Climat. Dynam.*, 27(2-3): 281-299. DOI: 10.1007/s00382-006-0125-9.
- 578 Rolland, C., 2003. Spatial and seasonal variations of air temperature lapse rates in  
579 alpine regions. *J. Climate*, 16(7):1032-1046. DOI: 10.1175/1520-0442(2003)016.
- 580 Shi, Y.F., Shen, Y.P., Hu, R.J., 2002. Preliminary study on signal, impact and foreground  
581 of climatic shift from warm-dry to warm-humid in northwest China. *Journal of*  
582 *Glaciology and Geocryol*, 24(3): 219-226.

- 583 Tao, H., Gemmer, M., Bai, Y., Su, B., Mao, W., 2011. Trends of streamflow in the Tarim  
584 River Basin during the past 50 years: Human impact or climate change?  
585 *J.Hydrol.*, 400(1-2):1-9. DOI: 10.1016/j.jhydrol.2011.01.016.
- 586 Vincent, L.A., Mekis, E., 2006. Changes in daily and extreme temperature and  
587 precipitation indices for Canada over the twentieth century. *Atmos.Ocean*, 44(2):  
588 177-193.
- 589 Wang, H.J., Chen, Y.N., Chen, Z.S., 2013a. Spatial distribution and temporal trends of  
590 mean precipitation and extremes in the arid region, northwest of China, during  
591 1960-2010. *Hydrol. Process.*, 27(12): 1807-1818. DOI: 10.1002/hyp.9339.
- 592 Wang, H.J., Chen, Y.N., Chen, Z.S., Li, W.H., 2013b. Changes in annual and seasonal  
593 temperature extremes in the arid region of China, 1960-2010. *Nat.Hazards*,  
594 65(3): 1913-1930. DOI: 10.1007/s11069-012-0454-4.
- 595 Wang, H.J., Chen, Y.N., Xun, S., Lai, D.M., Fan, Y.T., Li, Z., 2013c. Changes in daily  
596 climate extremes in the arid area of northwestern China. *Theor. Appl. Climatol.*,  
597 112(1-2): 15-28. DOI: 10.1007/s00704-012-0698-7.
- 598 Wang, Y., Chen, Y.N., Ding, J.L., Fang, G.H., 2014. Land-use conversion and its  
599 attribution in the Kaidu-Konqi River Basin, China. *Quatern. Int.*,  
600 <http://dx.doi.org/10.1016/j.quaint.2014.10.010>.
- 601 Xu, J., Chen, Y., Ji, M., Lu, F., 2008. Climate change and its effects on runoff of Kaidu  
602 River, Xinjiang, China: A multiple time-scale analysis. *Chinese Geogr. Sci.*,  
603 18(4): 331-339. DOI: 10.1007/s11769-008-0331-y.
- 604 You, Q., Kang, S., Pepin, N., Flügel, W. A., Yan, Y., Behrawan, H., Huang, J., 2010.  
605 Relationship between temperature trend magnitude, elevation and mean  
606 temperature in the Tibetan Plateau from homogenized surface stations and  
607 reanalysis data. *Global Planet. Change*, 71(1), 124-133.
- 608 You, Q. et al., 2011. Changes in daily climate extremes in China and their connection to  
609 the large scale atmospheric circulation during 1961–2003. *Climate Dynamics*,  
610 36(11-12), 2399-2417. DOI: 10.1007/s00382-009-0735-0.

611 Zhou, X., Chen, D.J.,1998. Study on vertical change features of climate in the southern  
612 slope of Tianshan Mountains [in Chinese with English abstract]. Journal of  
613 Mountain Science, 1: 47-52.

614 Zhou, Y.Q., Ren, G.Y., 2009. The effect of urbanization on maximum, minimum  
615 temperatures and daily temperature ranges in north China [in Chinese with  
616 English abstract]. Plateau Meteorology, 28(5):1158-1166.

617

618

619

620

621

622

623

624

625

626

627

628

629

630

631

632

633

634

635

636

637

638



639

640 Tables:

641 Table 1 Vertical region in the southern slope of the Tianshan Mountain (Zhou and Chen,

642 1998).

Region	Elevation(m)	Daily average temperature $\geq$ 5°C days (day)	Precipitation (mm)	Soil	Vegetation
Oasis	<1500	>210	<100	brown desert soil	desert shrub
Middle Mountain	1500-2200	210-150	150-300	brown desert soil brown calcic soil	semi-desert and desert grassland
High Mountain	2200-3100	150-70	no data	chestnut soil subalpine meadow soil	Alpine grassland
	3100-3600	70-40	no data	alpine meadow soil	alpine meadow
	>3600	<40	no data	primitive soil bare ice	cushion sparse vegetation

643

644

645

646

647

648

649

650

651

652

653

654

655

656 Table 2. List of selected stations, including three meteorological stations and one  
657 hydrological station

Station name	Latitude (°N)	Longitude (°E)	Elevation (m)	Period of record	Timescales	Annotation
Balguntay	42.73	86.3	1753	1958-2010	daily	Meteorological station
Bayanbulak	43.03	84.15	2458	1958-2010	daily	Meteorological station
Yanqi	42.08	86.57	1056	1952-2010	daily	Meteorological station
Heshou	42.25	86.8	1082	1960-2010	monthly	Meteorological station
Hejing	42.32	86.4	1067	1960-2010	monthly	Meteorological station
Dashankou	42.22	85.73	1340	1956-2010	daily	Hydrological station

658

659

660

661

662

663

664

665

666

667

668

669

670

671 Table 3. Temperature and precipitation indices

ID	Name	Definitions	Units
	Temperature indices		
TNn	Min Tmin	Monthly minimum value of daily minimum temperature	°C
TNm	Mean Tmin	Monthly mean value of daily minimum temperature	°C
TMn	Min Tmean	Monthly minimum value of daily mean temperature	°C
Tav	Mean Tmean	Monthly average value of daily mean temperature	°C
TMx	Max Tmean	Monthly maximum value of daily mean temperature	°C
TXm	Mean Tmax	Monthly mean value of daily maximum temperature	°C
TXx	Max Tmax	Monthly maximum value of daily maximum temperature	°C
FDO	Frost days	Annual count when daily minimum temperature $<0^{\circ}\text{C}$	days
IDO	Ice days	Annual count when daily maximum temperature $<0^{\circ}\text{C}$	days
SU25	Summer days	Annual count when daily maximum temperature $>25^{\circ}\text{C}$	days
GSL	Growing season Length	Annual (1 <sup>st</sup> Jan to 31 <sup>st</sup> Dec in NH, 1 <sup>st</sup> July to 30 <sup>th</sup> June in SH) count between the first span of at least 6 days with $\text{TG}>5^{\circ}\text{C}$ and the first span after July 1 (January 1 in SH) of 6 days with $\text{TG}<5^{\circ}\text{C}$	days
	Precipitation indices		
Pav	Precipitation total	Annual total PRCP on wet days ( $\text{RR}\geq 1\text{mm}$ )	mm
CWD	Consecutive wet days	Maximum number of consecutive days with $\text{RR}\geq 1\text{mm}$	days
CDD	Consecutive dry days	Maximum number of consecutive days with $\text{RR}<1\text{mm}$	days
R10	Number of heavy precipitation days	Annual count of days when $\text{PRCP}\geq 10\text{mm}$	days

672

673

674

675 Table 4. Trend analysis results of annual temperature indices (FDO, IDO, and SU25) in  
 676 the Kaidu River Basin. Mean  $\pm$  SE (day/a) are the mean of temperature indices  $\pm$   
 677 standard error (SE). Trend rate (day/a) was used to calculate the slopes of temperature  
 678 indices in the past 53 years. A Mann-Kendal test (Z) was used to detect the trends of  
 679 temperature indices.

Regions	Indices	Mean $\pm$ SE	Trend rate	Z value	Significance
Oasis	FDO	162 $\pm$ 9.26	-0.38	-5.37	***
	IDO	54 $\pm$ 11.48	-0.028	0.19	-
	SU25	127 $\pm$ 8.62	0.22	2.91	***
Middle	FDO	164 $\pm$ 13.54	-0.59	-4.68	***
Mountain	IDO	42 $\pm$ 11.71	-0.15	-1.4	-
	SU25	66 $\pm$ 10.21	0.23	2.37	**
High	FDO	260 $\pm$ 9.36	-0.37	-4.61	***
Mountain	IDO	139 $\pm$ 14.05	-0.22	-1.7	*
	SU25	1.1 $\pm$ 1.35	0.01	0.87	-

680 “\*” p<0.1; “\*\*” p<0.05; “\*\*\*” p<0.01

681

682

683

684

685

686

687

688

689

690

691 Table 5. The Pearson's correlation coefficient shows the season runoff, temperature  
 692 lapse rate, and mountain precipitation in the Kaidu River Basin. MAM are the months  
 693 of March to May, JJA are the months of June to August, SON are the months of  
 694 September to November, and DJF are the months of December to February of the  
 695 following year.

	MAM		JJA		SON		DJF	
	TLR	Precipitation	TLR	Precipitation	TLR	Precipitation	TLR	Precipitation
Runoff	0.28*	0.29*	0.09	0.75**	-0.37**	0.21	0.04	0.19

696 “\*” is  $p < 0.05$ ; “\*\*” is  $p < 0.01$ 

697

698

699

700

701

702

703

704

705

706

707

708

709

710

711

712

713 Figure Captions:

714

715 Figure 1. Study area and the meteorological and hydrological stations

716

717 Figure 2. Variability of daily temperature indices in the Kaidu River Basin. The black  
718 straight line (the reference line) indicates increases over this line and  
719 decreases under this line (from 1958 to 2010).

720

721 Figure 3. Variability of seasonal daily temperature indices in the Kaidu River Basin, A:  
722 summer daily temperature indices, B: winter daily temperature indices. The  
723 black straight line (the reference line) indicates increases over this line and  
724 decreases under this line (from 1958 to 2010).

725

726 Figure 4. The trends of Growing Season Length (GSL) in the high mountain region (A),  
727 middle mountain region (B), and oasis region (C) (from 1960 to 2010).

728

729 Figure 5. The percentage analysis of seasonal precipitation of three sub-regions (A,  
730 oasis region; B, middle mountain region; C, high mountain region) in the  
731 Kaidu River Basin, MAM (from March to May), JJA (from June to August),  
732 SON (from September to November), and JFD (January, February, and  
733 December in the same year). From top to bottom: results for Annual, MAM,  
734 JJA, SON, and JFD. From left to right: results for the oasis region, middle  
735 mountain region, and high mountain region.

736

737 Figure 6. The correlations of the annual precipitation with R10 and CWD from 1958 to  
738 2010 in the Kaidu River Basin. R10 is the annual number of days when  
739  $PRCP \geq 10\text{mm}$ ; CWD is the maximum number of consecutive days with  
740  $RR \geq 1\text{mm}$ .

741 Figure 7. The analysis results of mean temperature lapse rate in the Kaidu River Basin  
742 during the past 50 years: A is mean temperature lapse rate for observation  
743 stations data in the Kaidu River Basin during 1960-2010, and the solid line is  
744 the linear fit for all data; B is year-to-year variability in monthly-mean lapse  
745 rates, thick horizontal lines show the month's median lapse rate calculated  
746 using the observation station data in the Kaidu River Basin from 1958 to 2010,  
747 boxes show the inner-quartile range, the whiskers show the full range of the  
748 data, and red plus sign shows the extreme values.

749

750 Figure 8. The trend analysis of runoff in the Kaidu River Basin, A: the trends of annual  
751 and season runoff change in the Kaidu River Basin, MAM, JJA, SON, and  
752 JFD (January, February, and December in the same year); B: year-to-year  
753 variability in monthly mean runoff in the Kaidu River Basin during  
754 1956-2012.

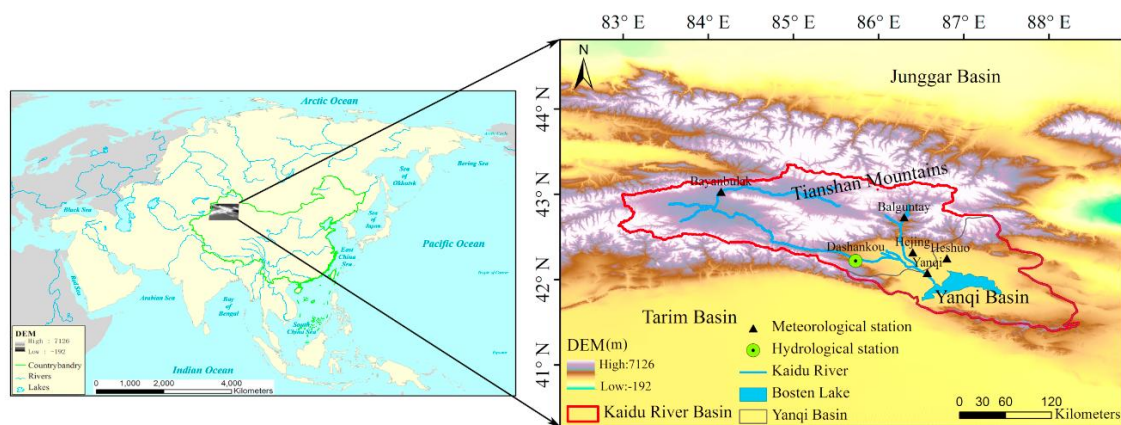
755

756 Figure 9. The comparison of the runoff with temperature lapse rates and annual  
757 precipitation in the Kaidu River Basin. The red line is runoff; the black lines  
758 are temperature lapse rates (A) and precipitation (B).

759

760 Figure 10. The cities and agricultural effects for the temperature change (A), and the  
761 city and agricultural contributions for the temperature change (B). The  
762 analysis results of city and agricultural effects and contributions are based on  
763 the equations in Section 2.3.4.

764

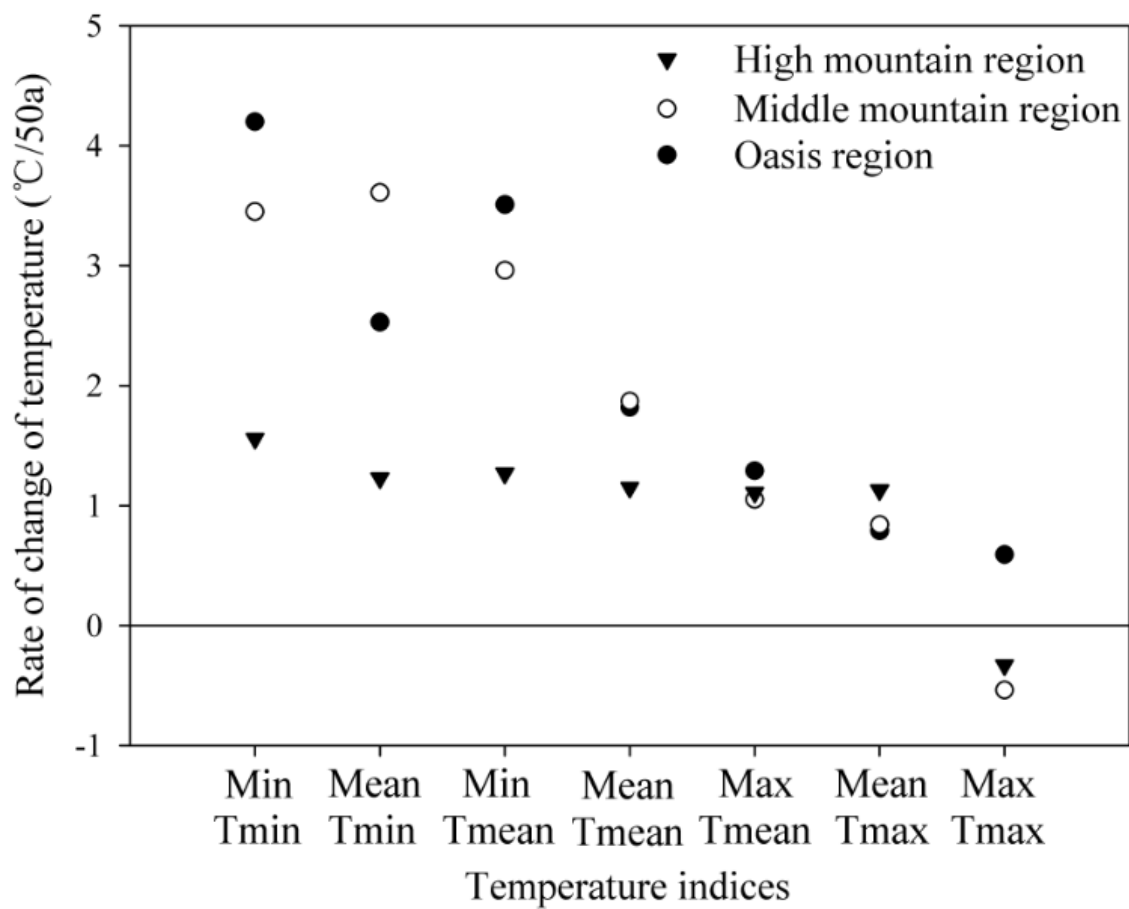


765

766 Fig. 1

767

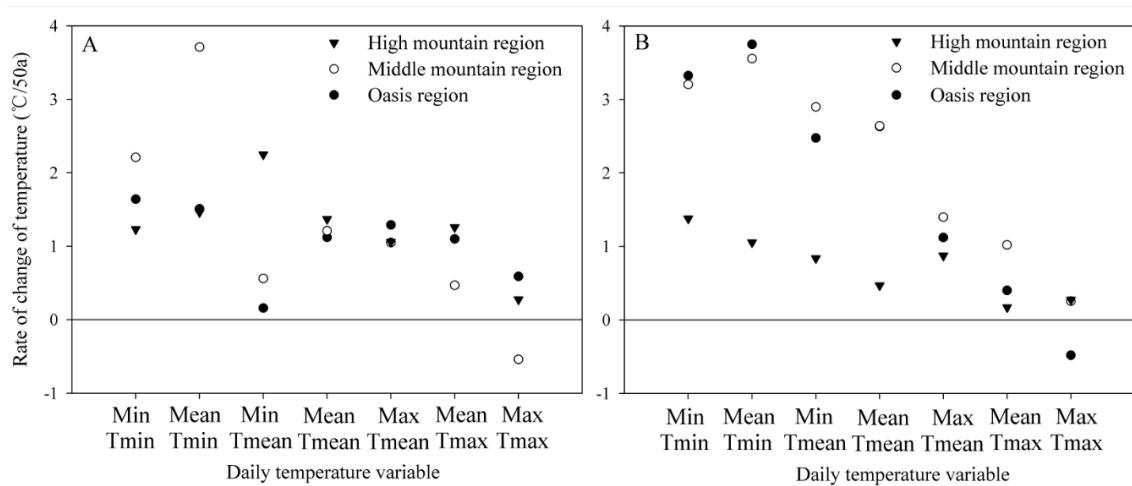




768

769 Fig. 2

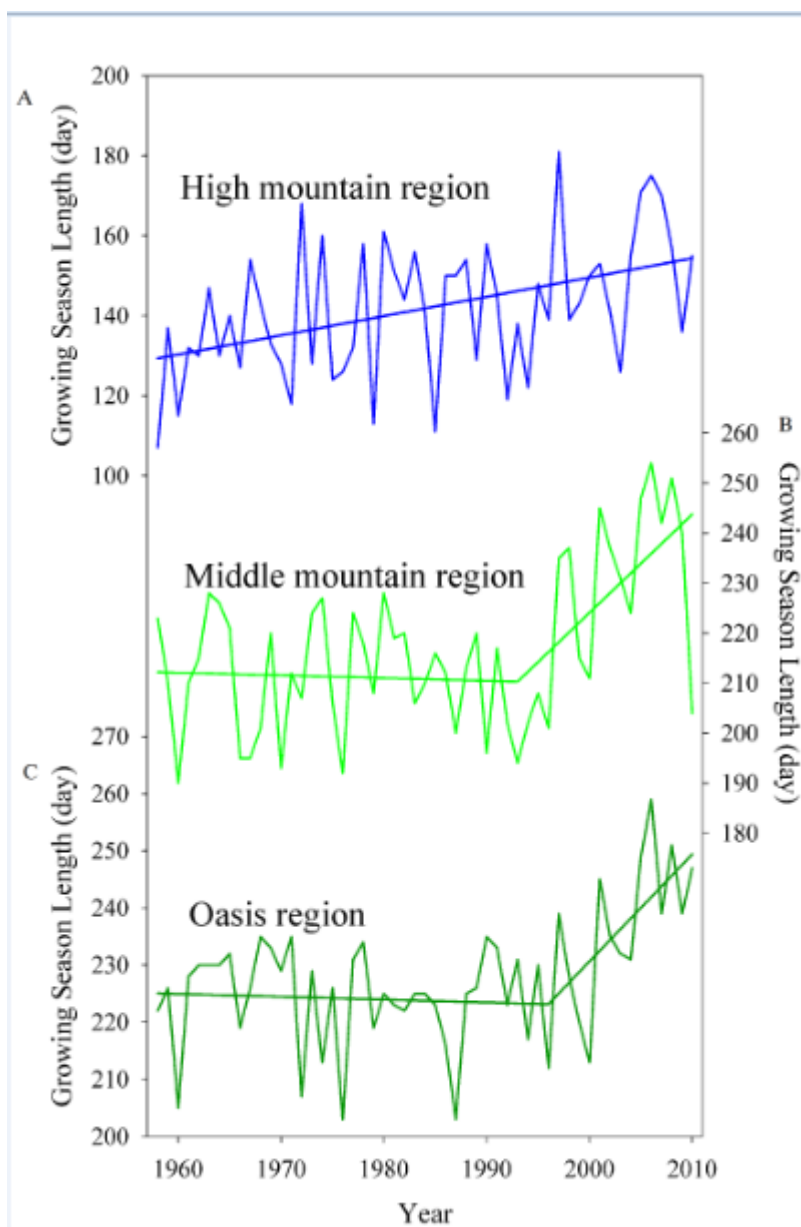
770



771

772 Fig. 3

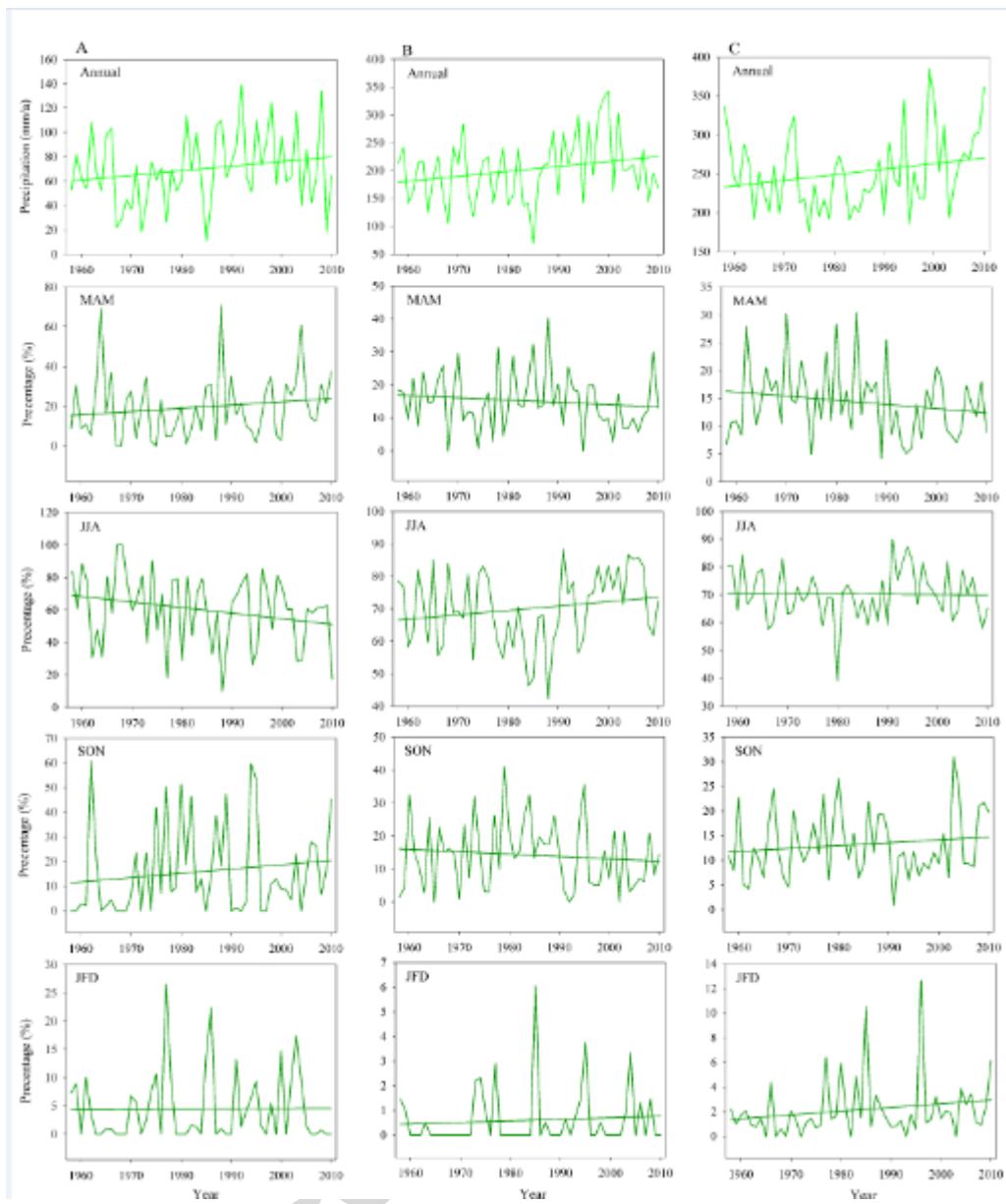
773



774

775 Fig. 4

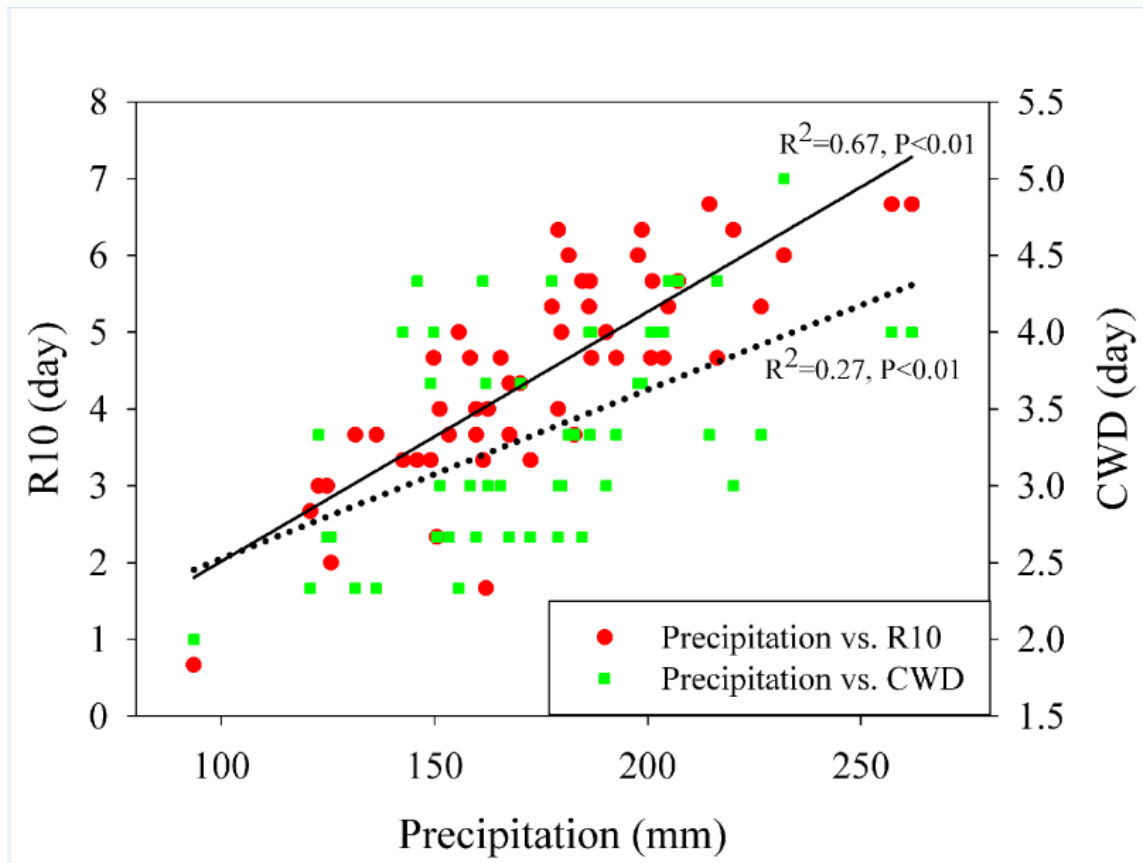
776



777

778 Fig. 5

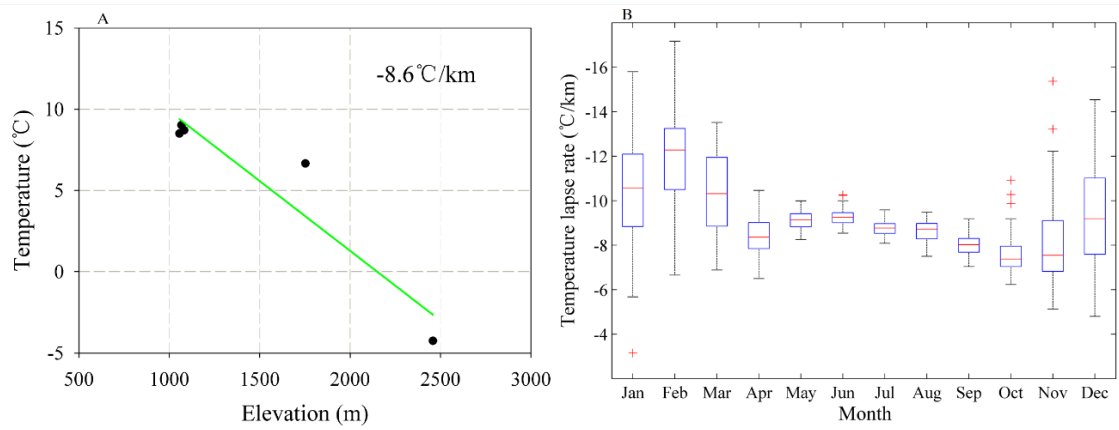
779



780

781 Fig. 6

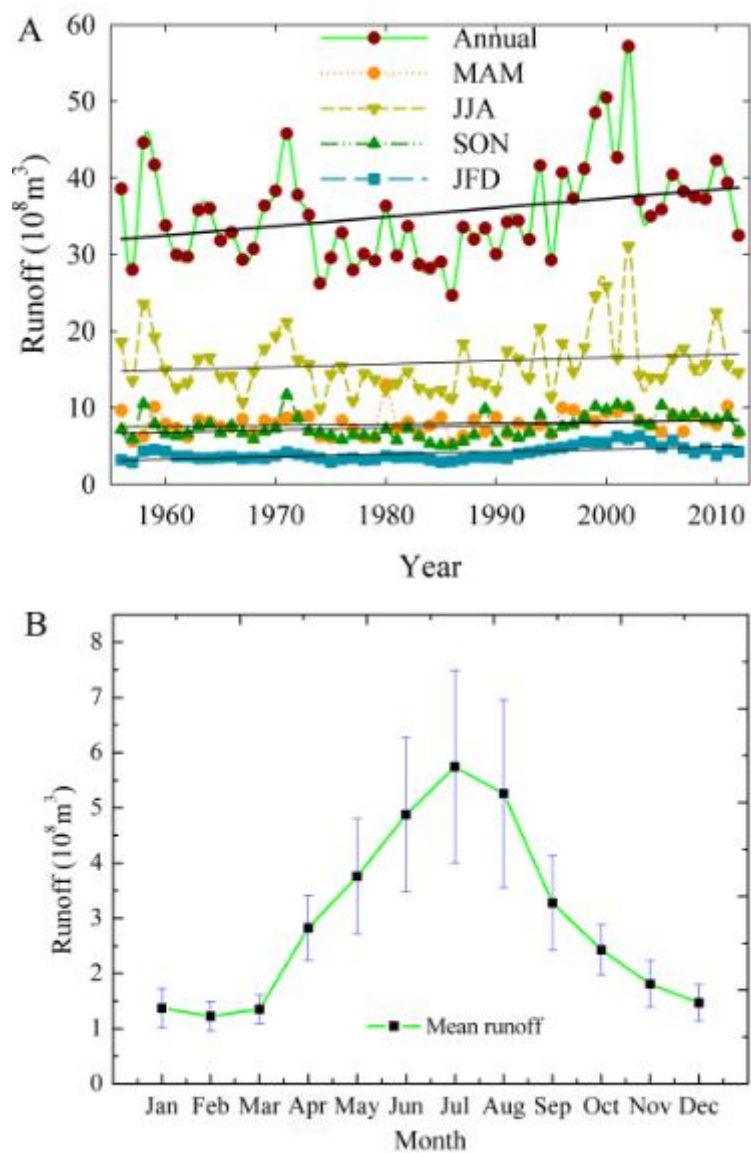
782



783

784 Fig. 7

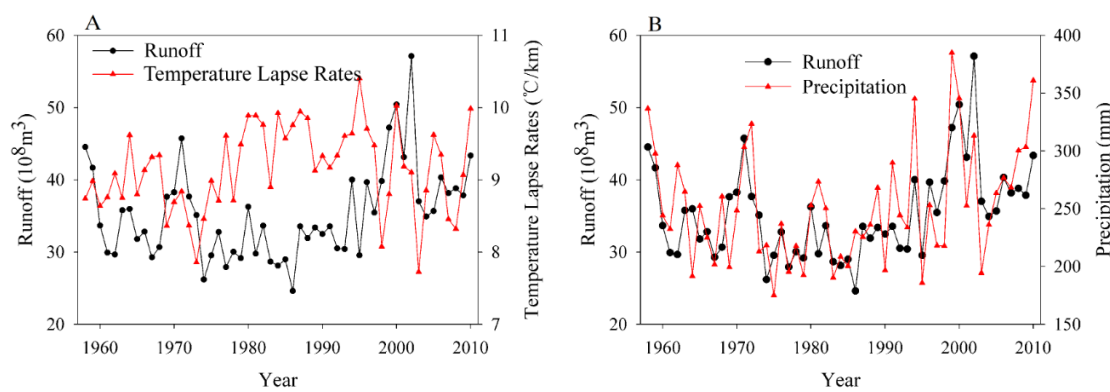
785



786

787 Fig. 8

788

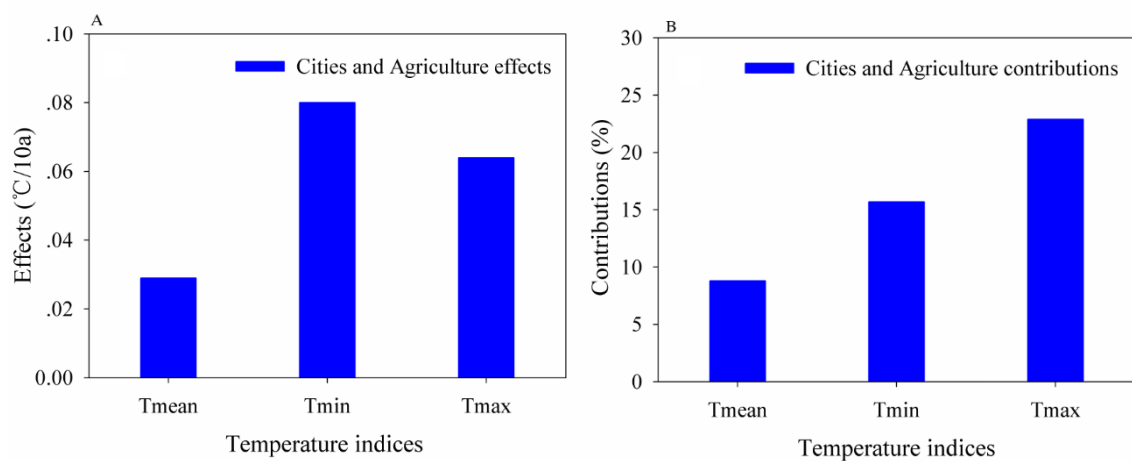


789

790 Fig. 9

791





792

793 Fig. 10

794

795 Highlights:

- 796 ● We discovered that temperature lapse rates have significant effects on runoff.
- 797 ● Rising rate of low temperature indices was larger than high temperature indices.
- 798 ● Increasing rate of temperature in the oasis region was higher than mountain region.
- 799 ● It was found that R10 and CWD contributed most to the increasing precipitation.

800

801

ACCEPTED MANUSCRIPT